Performance Enhancement of Two-Stage Corona Wind Generator in a Circular Pipe

G. D. Conanan and F. C. Lai
School of Aerospace and Mechanical Engineering
University of Oklahoma
phone: (1) 405-325-1748
e-mail: flai@ou.edu

***Abstract*- It is well known that an intense electric field generated between a sharp pointed conductor at a high voltage and a grounded electrode produces a flow of ionized air. The range of this electrically induced flow (known as the corona wind), however, may be limited to a confined region. This research proposes and investigates the concept of using multiple corona wind generators in series to extend the flow for a longer distance. To evaluate the performance of EHD gas pumps, separate experiments have been conducted to measure the velocity profiles of air flow induced by single- and two-stage corona wind generators. It has been found that additional stage can effectively increase the volumetric flow rate of corona wind generated by a single stage alone and extend its applicable range.**

INTRODUCTION

A corona wind is a stream of ionized fluid induced by a strong electric field. It is produced by an intense electric field between a sharp conductor charged at a high voltage and a grounded electrode in the presence of a dielectric medium that can be polarized by an applied electric field. To describe this phenomenon, consider a point-to-plane corona wind generator as shown in Fig. 1. It can be seen that a needle is used as the emitting electrode that is charged at a high voltage; a metal plate is used as the grounded electrode; and air is the dielectric medium in this particular example.

When a voltage is applied to the emitting electrode, an electric field is established between these two electrodes. When the voltage becomes high enough, which surpasses the ionization energy threshold, the intensified electric field at the sharp conductor will ionize the air nearby and form a corona on its surface. This corona is a gas discharge phenomenon resulting from the gas ionizing processes [1] and is known to glow at a violet-blue tint. This corona in turn sets the ionized air of the same polarity in motion towards the grounded plate [1] as shown in Fig. 2. These ions in motion, which are driven by Coulomb forces produced by the electric field, then collide with neutral gas molecules and transfer their momentum. This transfer of momentum results in a micro-jet flow issuing from the emitting electrode, which is also shown in Fig. 2.

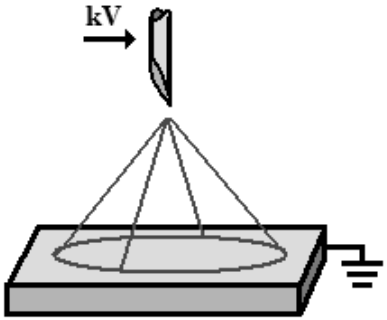

Fig. 1 A point-to-plane corona wind generator.

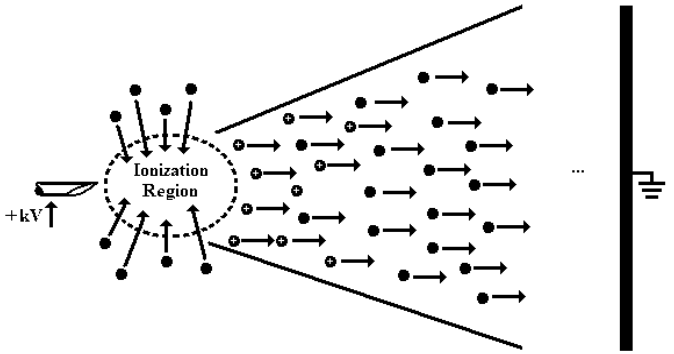

Fig. 1 Corona wind.

One feature associated with the corona discharge phenomenon that must be addressed is the possible occurrence of sparkover as the applied voltage increases. This is a spontaneous transformation of corona to spark that produces an undesirable increase in discharge current and a jump of charge in tandem with an intense flash occurring from the emitting electrode to the grounded electrode. Therefore, the range of voltages applied is usually recommended between the ionization and sparkover thresholds.

Other features of corona discharge have been considered critical in many applications. As a result, there have been numerous studies to further examine the various attributes of corona wind, optimize these distinct features, and utilize them in various applications. Corona wind, or a specific feature of corona wind, has been critically examined for its underlying physical principles [3-6, 16-20], applications in electronics cooling [7], flow control [8-11], and drying processes [12-15, 21-25].

One major commonality among various applications of corona wind is the design of electrode configuration so that corona wind can be manipulated to meet its specific need. An important consideration in the design of electrodes is the applicable range of corona wind, which determines how the device will be implemented in certain applications. The

flow of ionized fluid may be limited to a confined region since the required electric field is only established between the charged and grounded electrodes. This thus imposes serious constraints on the system design to accommodate the confined flow region. To improve the applicable range of corona wind in various applications, the current research proposes and investigates a novel way to sustain the flow of corona wind over a longer distance by using multi-stage generators.

To further demonstrate the idea of this research, consider a pin-to-plate corona wind generator installed on the inner surface of a circular pipe as shown in Fig. 3. This particular electrode configuration consists of an array of fine wire teeth to which a voltage is applied and a grounded electrode that is also mounted on the inner surface of the pipe at a distance away. This setup allows an externally driven flow, which in this case is shown to be a common Hagen-Poiseuille flow, to be enhanced by the corona discharge. This flow enhancement can be accomplished by the corona wind produced from the electrode on the inner surfaces, which disrupts the boundary layer established by the inlet flow. As a result, it induces flow at a higher velocity near the wall and leads to an enhancement in the volume flow rate. This enhancement, however, is only limited to the region where the corona wind can be felt by the flow. At the downstream of the grounded electrode, the flow may return to its original velocity profile established by the inlet flow. Although this electrohydrodynamically enhanced (EHD-enhanced) flow can be effectively initiated, its applicable range may be limited to a confined area. To overcome this limitation, a novel idea of using multi-stage electrodes to sustain the corona-induced flow for a longer distance and potentially continue the flow enhancement process is proposed and examined in this study.

The theory behind this multi-stage EHD gas pump is that the successive corona wind generator(s) may be able to take advantage of the flow already initiated from the preceding stage as a booster, which is shown in Fig. 4. The first stage generator induces corona wind as previously discussed. Once in motion, fluid particles will continue moving downstream, passing over the grounded plate in that stage. When these fluid particles enter the next stage, they receive additional energy from the local electric field, which sets them in an increased, or boost-liked, motion towards the grounded plate in this stage. Thus, it will sustain the corona-induced flow for a longer distance. If this were implemented in a system with an externally driven flow, the region containing the corona wind generator will see an improvement on the overall velocity profile and extend the applicable range of corona wind.

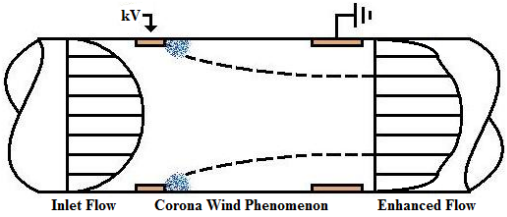

Fig. 2 A circular pipe with a corona wind generator.

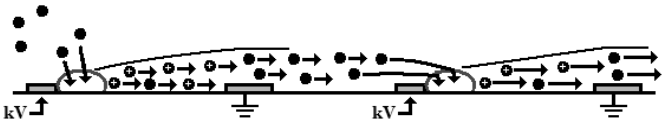

Fig. 4 A cross-sectional view of a two-stage EHD gas pump.

EXPERIMENTAL SETUP AND PROCEDURE

A. Experimental Setup

In this study, two sets of experiments have been conducted so that the feasibility and effectiveness of using multistage corona wind generator can be carefully evaluated. The first set of experiment was conducted to evaluate the performance of individual single-stage corona wind generator. The second set was to evaluate the performance of a combined system when two single-stage generators were assembled together. The two single-stage corona wind generators considered, as shown in Fig. 5, are made from 6.35-cm (2.5-inch) inner-diameter Plexiglas tube. The tube was machined to hold a ring of 24-gauge copper wire with four evenly spaced extruding teeth each of 1.27-cm (0.5-inch) long which were to serve as the emitting electrode, and a thin copper plate of 1.27-cm (0.5-inch) wide which was to serve as the grounded electrode. The placement of copper plate was respectively 1.27- and 2.54-cm (0.5- and 1-inch) downstream of the emitting electrode in the two single-stage corona wind generators considered.

Two DC high voltage power supplies (Bertan Associates, Series 205 B-30R) were used to produce the needed electric field. A hot-wire anemometer (Omega FMA 902-I) was used to measure the velocity of air flow induced by the corona wind generator. Velocity measurement was taken 6.35 cm (2.5 in.) downstream of the grounded electrode at selected radial locations. Since the velocity probe would interfere and modify the flow field, the velocity measurement through the entire cross-sectional might not necessarily provide more accurate information [34]. Thus it had been assumed that the velocity pro-

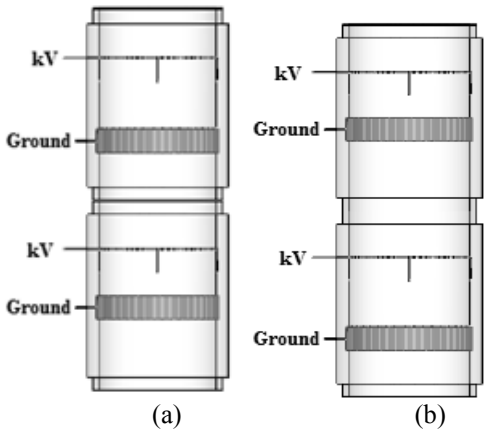

Fig. 5 A two-stage EHD gas pump: (a) Case 1, (b) Case 2.

file was axi-symmetrical and velocities were only measured in one radial direction from the pipe center to near the pipe wall. To facilitate the velocity measurement, a leveling and traversing device was designed and constructed in-house. The device allowed the distance between the edge of the closest grounded plate and the velocity transducer to be fixed at 6.35 cm (2.5 in.) and the radial locations of measurement point repeatable. A simple data acquisition unit NImyDAQ by National Instrument was used to collect signals produced from the velocity transducer and the power supply, and converted them into digital values with proper units using a LabVIEW program. Since corona discharge phenomenon is greatly influenced by the ambient conditions, a temperature and humidity data logger by Dickson (D200) has also been used to record the temperature and humidity of the ambient air during experiments.

The experimental setup is shown in Fig. 6. Since the electrode spacing was different in the two single-stage corona wind generators examined, the onset and sparkover voltages were also different between them. The generator with a shorter spacing (1.27-cm) had an onset voltage at 13 kV and sparkover at 18 kV while the one with a larger spacing (2.54-cm) saw an onset voltage around 22 kV and sparkover at 28 kV. The two- stage EHD gas pump was assembled from the two single-stage corona wind generators described earlier (Fig. 5). Case I has the generator with a 1.27-cm electrode-spacing on top and that of 2.54-cm spacing below while it is reversed for Case II. For both cases, the emitting electrodes (copper teeth) were perfectly aligned. Notice that two high voltage power supplies were employed in the test of two-stage corona wind generator. Each power supply was connected to individual one-stage generator. Thus, applied voltage to each single-stage corona wind generator could be adjusted independently.

RESULTS AND DISCUSSION

V-I curves of individual single-stage corona wind generator are shown in Fig. 7. As observed, corona current increases with an increase in the applied voltage. This trend is also reported in many previous studies [3-4, 6-7, 9-10, 13, 15, 18-20, 26-33]. Also noticed is that the onset voltage is smaller for the generator with a shorter electrode spacing

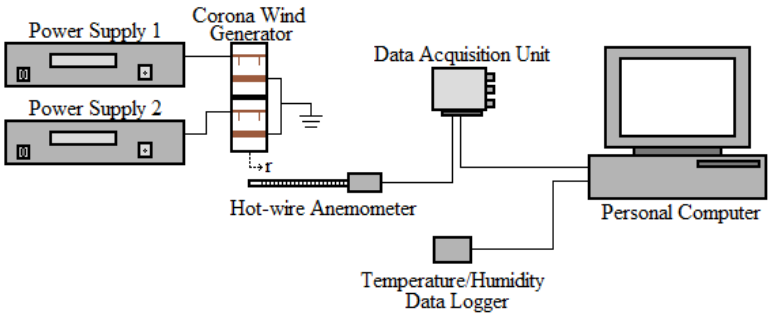

Fig. 3 Experimental setup.

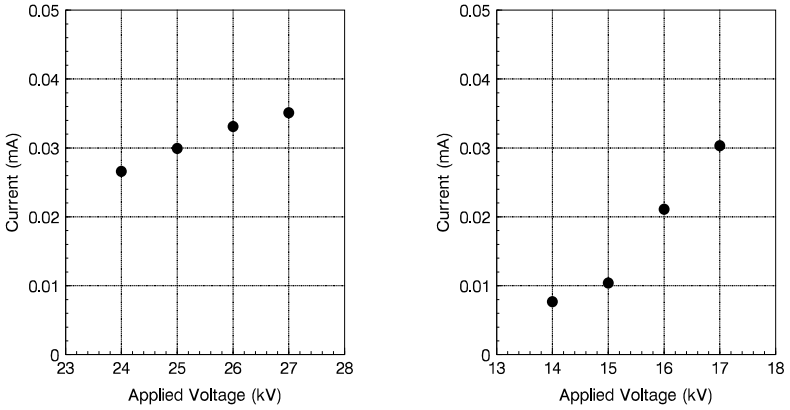

Fig. 7 V-I characteristics for a single-stage corona wind generator with (a) 2.54-cm electrode spacing, (b) 1.27-cm electrode spacing.

(1.27-cm). For the same corona current, one observes that the generator with a larger electrode spacing requires a higher voltage. In all cases, one notices that the corona current involved is very small (5-35 μA), which implies that the power required to initiate and maintain corona wind may also be consequently small. Indeed it was found that the power required for all cases considered in this study were below 1 mW which is significantly lower than those of conventional fan or pump. This finding demonstrates one of the salient features of corona wind generator for gas pumping.

The velocity profiles of corona-induced flow are shown in Fig. 8 for the two single-stage corona wind generators considered. As observed from these figures, the air veloc-

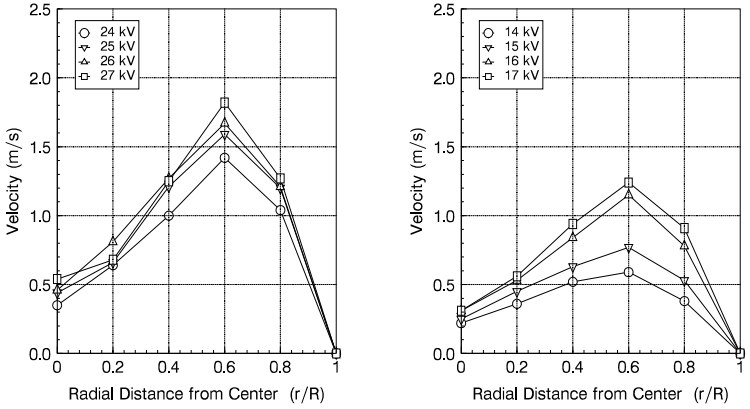

Fig. 8 Velocity profile of corona-induced air flow from a single-stage generator with electrode spacing of (a) 2.54-cm and (b) 1.27-cm.

ity at each sampling point becomes stronger as the applied voltage increases. This occurs because increasing the applied voltage strengthens the electric field intensity between the emitting pins and the grounded plate. The more intense the electric field strength is, the stronger the corona forms at the emitting electrode. This trend was also reported by other studies [19, 27-29]. It should be noted that each velocity profile has a maximum value close to the inner surface of the pipe and a minimum toward the centerline. This phenomenon is due to the fact that the emitting electrodes were mounted on the inner surface of the pipe wall. Since there was no flow driven externally, the only flow presented was the one induced by corona wind from the emitting electrodes. Thus the corona-induced flow behaved like a wall jet. Because of the presence of wall and fluid's viscosity, no-slip condition still applies. But the flow was channeled through a narrow region near the wall with a maximum velocity occurred near the inner surface of the pipe and a minimum velocity at the center. Also noticed, the generator with a smaller spacing between two electrodes (1.27-cm) requires a smaller applied voltage to achieve the same air velocity as that of the larger one. This occurs simply because the electric field intensity inside the pipe is dependent on the spacing between the two electrodes. As the gap distance decreases, the electric field intensity increases, which in turn produces a stronger corona wind.

Velocity profiles of corona-induced air flow by two-stage generators are shown in Fig. 9. For performance evaluation, measurements were taken first with the booster (the generator on top) being powered off, then both generators were powered on. For comparison, the velocity profiles with the booster being powered off were shown by symbols connected with a dashed line while those produced by both generators being powered on with the symbols alone. For both cases, when the booster (top) stage was powered off, one observes that the velocity profile of induced air flow was nearly identical to that produced by the corresponding single-stage generator. For Case I (the generator with a lar-

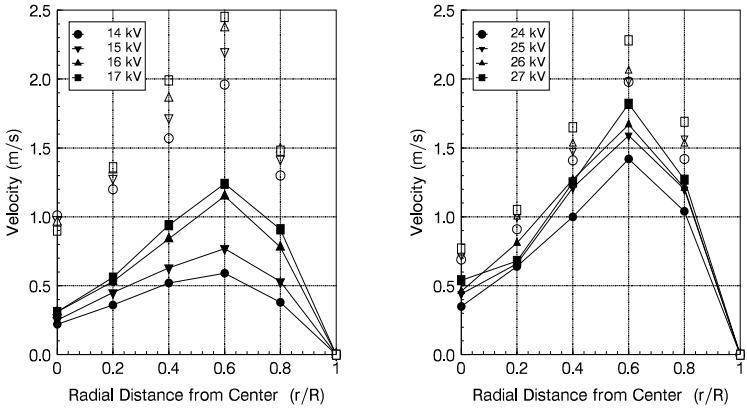

Fig. 9 Velocity profile of corona-induced air flow from a two-stage generator, (a) Case I and (b) Case II.

ger spacing on top), when the applied voltage to the booster stage was at 27 kV, air velocity was greatly increased (Fig. 9 (a)). However, the resulting air velocity was not exactly the sum of velocities produced from two individual single-stage corona generators. It is observed that the air velocity near the core region is more than the sum of velocities produced from two individual generators. On the other hand, the air velocity near the wall is less than that of the velocity sum. Apparently, some flow re-alignment took place between the two stages. Although the magnitude of velocity has changed, the velocity profile remains much the same as that produced by a single-stage generator. For Case II (the generator with a smaller spacing on top), one observes that the increase in air velocity was not as dramatic as the previous case when the applied voltage to the booster stage was at 17 kV. The resulting air velocity is generally smaller than the sum of velocities produced by two individual corona wind generators (Fig. 9 (b)). The reason why the increase in the induced air velocity from Case II was not as significant as that of Case I can be attributed to the distance between the grounded electrode of the booster stage and the emitting electrode of the primary stage. As one can see from Fig. 4, the distance between these two electrodes was shorter for Case I than that of Case II. As a result, air flow induced by the booster stage from Case I could reach the primary stage without loosing much of its momentum before it was recharged by the electric field in the second stage.

With the velocity data available, one can calculate the corresponding volume flow rate delivered by an EHD gas pump (either single-stage or two-stage). Using area as the weighting factor, one can calculate the volume flow rate of induced air flow, and which is shown in Fig. 10. As one observes, the volume flow rate of air induced by both cases of two-stage corona wind generator considered increases with the voltage applied to the bottom (primary) stage of the corona wind generator. One further observes that the volume flow rate of Case I (the generator with a larger spacing on top) increases with an increase in the voltage applied to the booster stage (Fig. 10 (a)). However, the volume flow rate of Case II (the generator with a smaller spacing on top) does not vary signify-

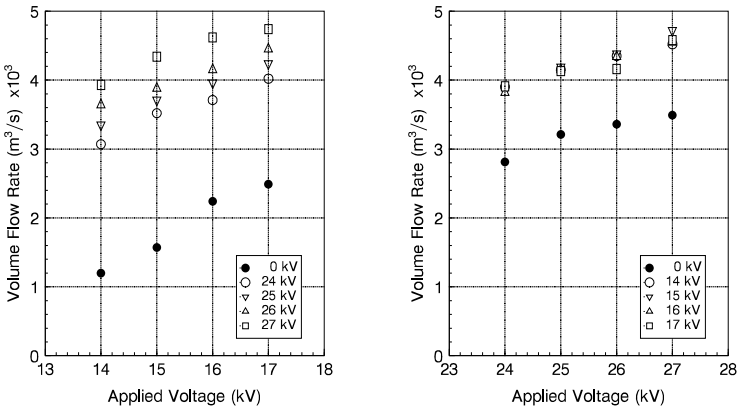

Fig. 10 Volume flow rate of air induced by two-stage EHD gas pump, (a) Case I and (b) Case II.

cantly with the applied voltage to the booster stage (Fig. 10 (b)). As discussed earlier, the resulting air velocity from the Case II of the two-stage EHD gas pump was not significantly enhanced by the booster stage due to the distance between its grounded electrode of the first stage and the emitting electrode of the second stage. As a result, the corresponding volume flow rate is also less affected by the voltage applied to the booster stage in Case II.

From Fig. 10, one important lesion is learned. That is, when using a multi-stage EHD gas pump, one needs to consider the gap distance between two neighboring stages. It will be more effective if one uses a corona wind generator with larger electrode spacing as the booster. In this arrangement, the corona-induced air flow from the first stage can reach the subsequent stage(s) without loosing much of its momentum due to flow disruption and realignment.

CONCLUSION

Experiments have been conducted to evaluate the feasibility of using multi-stage corona wind generator for gas pumping. The following are the conclusions that one can draw from the present study.

1. The power required to initiate and maintain a corona-induced flow is generally small as compared with most of the conventional fans.
2. The corona-induced flow has a maximum velocity occurs close to the inner surface of the pipe and a minimum velocity at the center of the pipe.
3. The volume flow rate of air produced by a two-stage generator increases as the voltage applied to the primary (bottom) stage increases.
4. The volume flow rate of air induced by a multi-stage corona wind generator is greater than that produced by an individual single generator, but smaller than the sum of them.
5. For a two-stage corona wind generator arranged in Case I (the generator with a large electrode spacing on top), the volume flow rate of air induced increases with an increase in the voltage applied to the booster (top) stage.
6. For a two-stage corona wind generator arranged in Case II (the generator with a smaller electrode spacing on top), the volume flow rate of air induced does not vary significantly with an increase in the voltage applied to the booster (top) stage.

The conclusions obtained from the present study have an important implication for the application of EHD gas pumps. That is, when using a multi-stage corona wind generator, it is more effective to use a generator with a larger electrode spacing as the booster as this arrangement can better sustain the corona-induced flow from the booster stage to the primary stage without much loss due to flow disruption and realignment.

ACKNOWLEDGMENTS

The authors would like to acknowledge the partial support for this study provided by the Undergraduate Research Opportunities Program (UROP) of the Honors College of the University of Oklahoma. The technical assistance provided by Professor John E. Fa-

gan and Mr. Clifford Morris (both of the School of Electrical and Computer Engineering) in circuit design and data acquisition is also gratefully acknowledged.

REFERENCES

[1] M. Goldman, A. Goldman, R. S. Sigmond, *The Corona Discharge, Its Properties and Specific Uses*, Pure & Applied Chemistry, Vol. 57, pp. 1353-1362, 1985.

[2] Y. Nikiforov, C. Leys, *Breakdown Process and Corona to Spark Transition between Metal and Liquid Electrodes*, Czechoslovak Journal of Physics, Vol. 56, 2006.

[3] M. Rickard, D. Dunn-Rankin, F. Weinberg, F. Carleton, *Characterization of ionic wind velocity*, Journal of Electrostatics, Vol. 63, pp. 711-716. 2005.

[4] X. Meng, H. Zhang, J. Zhu, *A General Empirical Formula of Current-Voltage Characteristics for Point-to-Plane Geometry Corona Discharges*, Journal of Physics D: Applied Physics, Vol. 41, pp. 1-10, 2008.

[5] G. W. Penney, S. E. Craig, *Sparkover as Influenced by Surface Conditions in D-C Corona*, AIEE, Paper 60-103, 1960.

[6] B. Komeili, J. S. Chang, G. Harvel, *Polarity Effect and Flow Characteristics of Wire-Rod Type Electrohydrodynamic Gas Pump*, 2006 Annual Report Conference on Electrical Insulation and Dielectric Phenomena, pp. 182-185, 2006.

[7] C. Hsu, N. E. Jewell-Larsen, I. A. Krichtafovitch, S. W. Montgomery, J. T. Dibene, A. V. Mamishev, *Miniaturization of Electrostatic Fluid Accelerators*, Journal of Microelectromechanical Systems, Vol. 16, pp. 809-815, 2007.

[8] P. Magnier, D. Hong, A. Leroy-Chesneau, J. Pouvesle, J. Hureau, *A DC Corona Discharge on a Flat Plate to Induce Air Movement*, Journal of Electrostatics, Vol. 65, pp. 655-659, 2007.

[9] E. Moreau, L. Leger, G. Touchard, *Effect of a DC Surface-Corona Discharge on a Flat Plate Boundary Layer for Air Flow Velocity Up to 25 m/s*, Jounal of Electrostatics, Vol. 64, pp. 215-225, 2005.

[10] K. T. Hyun, C. H. Chun, *The Wake Flow Control Behind a Circular Cylinder Using Ion Wind*, Experiments in Fluids, Vol. 35, pp. 542-552, 2005.

[11] J. R. Roth, *Aerodynamic Flow Acceleration Using Paraelectric and Peristaltic Electrohydrodynamic Effects of a One Atmosphere Uniform Glow Discharge Plasma*, Physics of Plasmas, Vol. 10, pp. 2117-2126, 2003.

[12] B. Hesse, *Energy Efficient Electric Drying Systems for Industry*, Drying Technology, Vol. 13, pp. 1543-1562, 1995.

[13] S. E. Sadek, R. G. Fax, M. Hurwitz, *The Influence of Electric Fields on Convective Heat and Mass Transfer from a Horizontal Surface under Forced Convection, Journal of Heat Transfer*, Vol. 94, pp. 144-148, 1972.

[14] Kirschvink-Kobayashi, J. L. Kirschvink, *Electrostatic Enhancement of Industrial Drying Processes*, Industrial & Engineering Chemistry Process Design and Development, Vol. 25, pp. 1027-1030, 1986.

[15] A. Wolny, R. Kaniuk, *The Effect of Electric Field on Heat and Mass Transfer*, Drying Technology, Vol. 14, pp. 195-216, 1996.

[16] M. M. Khalifa, R. M. Morris, *A Laboratory Study of the Effects of Wind on DC Corona*, IEEE Transactions on Power Apparatus and Systems, Vol. 86, pp. 290-296, 1967.

[17] N. L. Allen, Y. Teisseyre, P. Ballereau, M. Goldman, *Electrical Wind and Ionic Species Formed by Point-Plane Corona*, in Proceedings of the Sixth International Conference on Gas Discharges and Their Applications (Institution of Electrical Engineers), pp. 150–152. 1980

[18] H. Kawamoto, S. Umezu, *Electrohydrodynamic Deformation of Water Surface in a Metal Pin to Water Plate Corona Discharge System*, Journal of Physics D: Applied Physics, Vol. 38, pp. 887-894, 2005.

[19] H. Tsubone, J. Ueno, B. Komeili, S. Minami, G.D. Harvel, K. Urashima, C. Y. Ching, J. S. Chang, *Flow Characteristics of Dc Wire-Non-Parallel Plate Electrohydrodynamic Gas Pumps*, Journal of Electrostatics, Vol. 66, pp. 115-121, 2008.

[20] J. S. Chang, H. Tsubone, Y. N. Chun, A. A. Berezin, K. Urashima, *Mechanism of Electrohydrodynamically Induced Flow in a Wire-Non-Parallel Plate Electrode Type Gas Pump*, Journal of Electrostatics, Vol. 67, pp. 335-339, 2009.

[21] A. Wolny, *Intensification of the Evaporation Process by Electric Field*, Chemical Engineering Science, Vol. 47, pp. 551-554, 1992.

[22] H. R. Carlon, J. Latham, *Accelerated Drying of Water-Wetted Materials in Electric Fields*, Journal of Atmospheric and Terrestrial Physics, Vol. 56, pp. 487-492, 1994.

[23] H. R. Carlon, J. Latham, *Enhanced Drying Rates of Wetted Materials in Electric Fields*, Journal of Atmospheric and Terrestrial Physics, Vol. 54, pp. 117-118, 1992.
[24] Sumorek, W. Pietrzyk, *The influence of Electric Field on the Energy Consumption of Convective Drying Processes*, Agricultural Engineering International: the CIGR Journal of Scientific Research and Development, Manuscript FP 00 017, Volume III, 2001.
[25] N. N. Barthakur, N. P. Arnold, *Evaporation Rate Enhancement of Water With Air Ions from a Corona Discharge*, International Journal of Biometeorology. Vol. 39, pp. 29-33, 1995.
[26] M. Molki, M. M. Ohadi, *Heat Transfer Enhancement of Airflow in a Channel Using Corona Discharge*, Journal of Enhanced Heat Transfer, Vol. 7, pp. 411-425, 2000.
[27] Komeili, J. S. Chang, G. D. Harvel, C. Y. Ching, D. Brocilo, *Flow Characteristics of Wire-Rod Type EHD Gas Pump Under Negative Corona Operations*, Journal of Electrostatics, Vol. 66, pp. 342-353, 2008.
[28] E. Moreau, G. Touchard, *Enhancing the Mechanical Efficiency of Electric Wind in Corona Discharges*, Journal of Electrostatics, Vol. 66, pp. 33-44, 2008.
[29] H. Kalman, E. Sher, *Enhancement of Heat Transfer by Means of a Corona Wind Created by a Wire Electrode and Confined Wings Assembly*, Journal of Applied Thermal Engineering, Vol. 21, pp. 265-282, 2001.
[30] H. Kawamoto, S. Umezu, *Electrohydrodynamic Deformation of Water Surface in a Metal Pin to Water Plate Corona Discharge System*, Journal of Physics D: Applied Physics, Vol. 38, pp. 887-894, 2005.
[31] T. Goodenough, P. W. Goodenough, S. M. Goodenough, *The Efficiency of Corona Wind Drying and its Application to The Food Industry*, Journal of Food Engineering, Vol. 80, pp. 1233-1238, 2007.
[32] K. Yamada, *An Empirical Formula for Negative Corona Discharge Current in Point-Grid Electrode Geometry*, Journal of Applied Physics, Vol. 96, pp. 2472-2475, 2004.
[33] N. E. Jewell-Larsen, E. Tran, I. A. Krichtafovitch, A. V. Mamishev, *Design and Optimization of Electrostatic Fluid Accelerators*, IEEE Transactions on Dielectrics and Electrical Insulation, Vol. 13, pp. 191-203, 2006.
[34] J. Zhang and F. C. Lai, *Effects of Emitting Electrode Number on the Performance of EHD Gas Pump in a Rectangular Channel*, Journal of Electrostatics, Vol. 69, pp. 486-493, 2011.